CSCE Annual Conference
Growing with youth – Croître avec les jeunes

Laval (Greater Montreal)
June 12 - 15, 2019

LATERAL–TORSIONAL BUCKLING IN WELDED GIRDERS: PREDICTION AND MEASUREMENT OF RESIDUAL STRESSES

Daniel R. Unsworth[1,2], Leijun Li[1] and Robert G. Driver[1]
[1]University of Alberta, Canada
[2]Drunswor@ualberta.ca

Abstract: Lateral–torsional buckling (LTB) is a potential mode of failure for steel beams involving a combination of weak-axis and torsional buckling resulting from strong-axis bending. Canadian design standards CSA S6 and S16 specify checks that originated from the study of rolled steel beams to ensure they are designed to resist this failure mode. Recent studies suggest that the Canadian standards may overestimate the LTB capacity of welded beams; however, it is not clear that the residual stress distributions assumed are representative of girders in use today. For this reason, data from modern girders must be collected and examined. As part of an ongoing study, residual stress measurements on a series of eleven reduced-scale test girders will be conducted. Results obtained from the first girder specimen are reported and compared with a residual stress model proposed by Cherneko and Kennedy in 1991. Measured stress magnitudes are found to be over-predicted by the model, while the distribution of tensile and compressive regions, though accurate for the tested specimen, becomes less accurate for the flanges as flange width decreases, as shown by an examination of additional residual stress data from the literature.

1 INTRODUCTION

Lateral–torsional buckling (LTB) is a potential failure mode of steel beams involving a combination of weak-axis and torsional buckling resulting from strong-axis bending. Current Canadian design standards specify checks to ensure beams are designed to resist this failure mode; however, no distinction is made between rolled and welded sections (CSA 2014a, 2014b). While significant differences in residual stress distributions exist between the two types (potentially resulting in a lower inelastic buckling capacity), the difference has often been considered minimal with no distinction required for design. A recent study has shown that this practice may be unconservative: an analysis of multiple LTB tests found that while the current design curve yields a reliability index of 3.0 for rolled sections, the index for welded sections is only 1.6 (MacPhedran and Grondin 2011). It should be noted, however, that the test data used for that study came from experiments done from 1970 – 80 in Asia and Europe and may not be representative of beams and girders in use in Canada today. Relatively little data is available for modern welded girders; this project aims to gather data on a range of welded girders fabricated using modern welding procedures in order to assess the safety of the current design standard.

Data gathered comprises both physical LTB tests and residual stress measurements. Physical tests will provide a direct assessment of LTB capacity, while residual stress data will be used to facilitate a broader understanding of the results and ensure broad applicability of test results. This paper will present findings from residual stress measurements on the first specimen in the testing program.

2 PREVIOUS WORK

Much work was done to characterize residual stresses in structural steel sections at Lehigh University from 1948 – 1973 as part of an investigation into column stability. It was found that plate geometry and plate manufacture method are important influences on the resulting residual stress distribution, while the type of weld and base material yield stress are less important (Alpsten and Tall 1970). Data from selected Lehigh University tests were summarized by Cherneko and Kennedy and two simplified distributions proposed to facilitate use in numerical models—one for shapes fabricated using milled plates and one for those comprising flame-cut plates (Chernenko and Kennedy 1991). The simplified distribution for flame-cut plates is shown in Figure 1a.

In 1981, measurements on a series of 34 welded beams of nominally identical cross-section were completed as part of a larger study on LTB (Fukumoto and Itoh 1981). The mean distribution (shown schematically in Figure 1 (b)) was reported along with the standard deviation among the beams considered. A comparison was done with an earlier, similar testing program by Fukumoto et al. (1980) on rolled beams: mean ultimate capacity was found to be lower in the welded beams compared to that of the rolled beams. It was also observed that variation in both residual stresses and ultimate strength among beams was greater in the welded specimens.

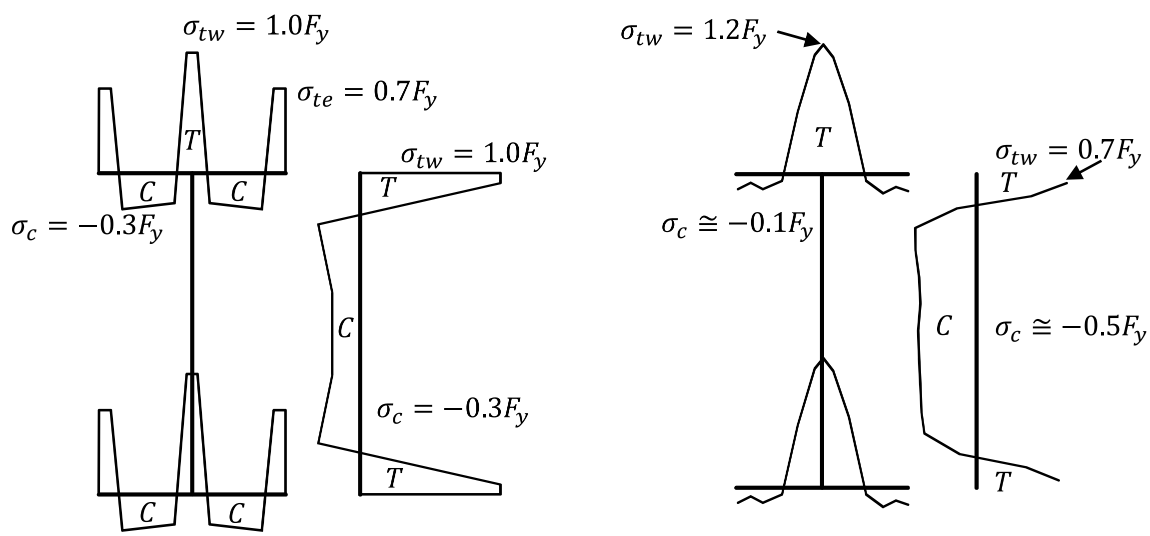

(a) (b)

Figure 1: Residual stress distributions from Cherneko and Kennedy (flame-cut plates) (a), and Fukumoto and Itoh (b)

A recent numerical study by Kabir and Bhowmick (2018) on LTB used distributions based on Cherneko and Kennedy's distributions and Fukumoto and Itoh's measurements as input residual stresses in a finite-element model. A range of wide-flange sections were modelled with depths ranging from 700 to 1800 mm, flange widths from 300 to 550 mm and plate thicknesses of 11 to 50 mm. Capacities were found to be up to 37% lower than those predicted by CSA S16. Of the stress distributions used, the Cherneko and Kennedy distribution for milled plates was found to yield the lowest capacity while that measured by Fukumoto and Itoh yielded the highest. This was attributed to the large tensile region in both flanges for the Fukumoto and Itoh distribution which significantly delays onset of yielding in the compression flange (Kabir and Bhowmick 2018).

3 METHODS

The testing program comprises a set of eleven welded steel girders fabricated from flame- or plasma-cut plates. All plates were Grade 350W steel—material properties are shown in Table 1. Yield stress values are as reported in the mill test report, while Young's modulus values were obtained from tension calibration tests of an ultrasonic stress-measurement system. Tension coupon tests will be conducted in the future to obtain more accurate values. Girders were fabricated using submerged-arc welding; plates were joined using single-pass fillet welds on both sides of the web. Welding data is shown alongside cross-sectional dimensions in Table 2 and Figure 2. Results from the testing of the first specimen (SP2-2A) are presented in this paper.

Table 1: Material properties

Plate thickness (mm)	σ_y (MPa)	E (GPa)
13	420	198
32	386	210

Table 2: Cross-sectional dimensions and welding parameters for specimen SP2-2A

	Cross-section dimensions				*Welding Parameters*				
Specimen	b *(mm)*	t *(mm)*	d *(mm)*	w *(mm)*	*V (V)*	*I (A)*	*speed (mm/s)*	*a (mm)*	*Plate cutting method*
SP2-2A	422	32	594	d	36	500	5.9	9	Flame-cut

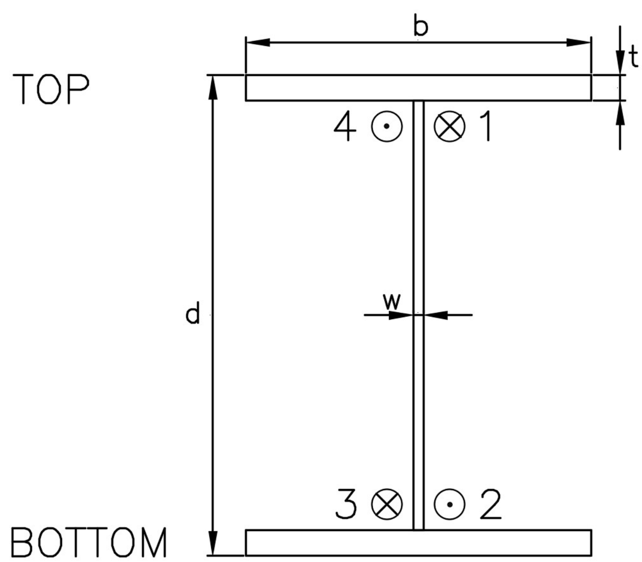

Figure 2: Cross-section and weld sequence information

3.1 Sectioning

The method of sectioning was used for residual stress measurements. First proposed by Kalakoutsky (1888), the modern procedure was largely developed through residual stress testing at Lehigh University from 1948 – 1973, with Tebedge et al. (1973) publishing documented procedures. A technical memorandum published by the Structural Stability Research Council (SSRC)(Pekoz et al. 1981) outlines the method of Tebedge et al. with minor modifications. The SSRC memorandum was used as the primary reference for sectioning procedures, with some modifications made due to laboratory capacity.

The sectioning method relies on release of elastic stresses: when a section of a sample containing residual stresses is removed, stresses in the removed section are released and changes in length are observed in the directions of stress release. If these changes in length are measured, separation of a girder into a series of longitudinal strips may be used to determine the longitudinal residual stress distribution over the girder cross-section.

A series of 30 mm wide strips were laid out at the centre of a 3 m long girder and two ball bearings were punched 100 mm apart at the centre of each strip. This was performed for both sides of each strip on the flanges, but only one side for the web, as through-thickness stress gradient is not expected to be significant for the web as plate thickness is less than one inch (Alpsten and Tall 1970). A stress-measuring extensometer was used to measure the distance between ball bearings prior to sectioning of the specimen. The device possesses a 100 mm gauge length and 1 μm resolution, allowing for a 2 MPa stress resolution in steel (if Young's Modulus = 200 GPa).

A 400 mm long sectioning piece was then removed from the centre of the girder with an oxy-acetylene torch. While the minimum sectioning piece length specified in the SSRC memorandum is 245 mm for 32 mm thick plates, extra distance was added to ensure heat input from flame cutting would not disturb residual stresses within the gauge length.

A water-cooled band saw was then used to separate the sectioning piece into strips. Following sectioning, distances between each pair of ball bearings were measured using the stress-measuring extensometer and the released stress for each strip was calculated using Equation 1, where E is the base material Young's modulus and L_i and L_f are the initial and final strip lengths, respectively. Strips from the specimen flanges after sectioning are shown in Figure 3.

[1] $\sigma = E(L_i - L_f)/L_i$

Figure 3: Flanges from specimen SP2-2A following sectioning

Strip curvature was also measured both before and after sectioning, as significant curvature of strips will result in a discrepancy between chord length of the strip (which the extensometer measures) and arc length (required for strain calculations). Various methods exist to correct the extensometer reading if curvature is significant; however, the magnitude of such corrections was found to be less that the resolution of the stress-measuring extensometer and thus corrections were not required.

4 RESULTS

4.1 Sectioning

Results from sectioning are shown in Figure 4 for both flanges and the web. Measurements on the interior face of the flanges are discontinuous between the two points on either side of the web due to the presence of the welds and web. Distributions are, broadly speaking, typical of a welded wide-flange girder: A narrow area of high tensile stress is present around the welded flange-web junction with the rest of the section in compression. Tensile stresses due to flame cutting are also observed at the edges of the flanges, though only on the exterior faces.

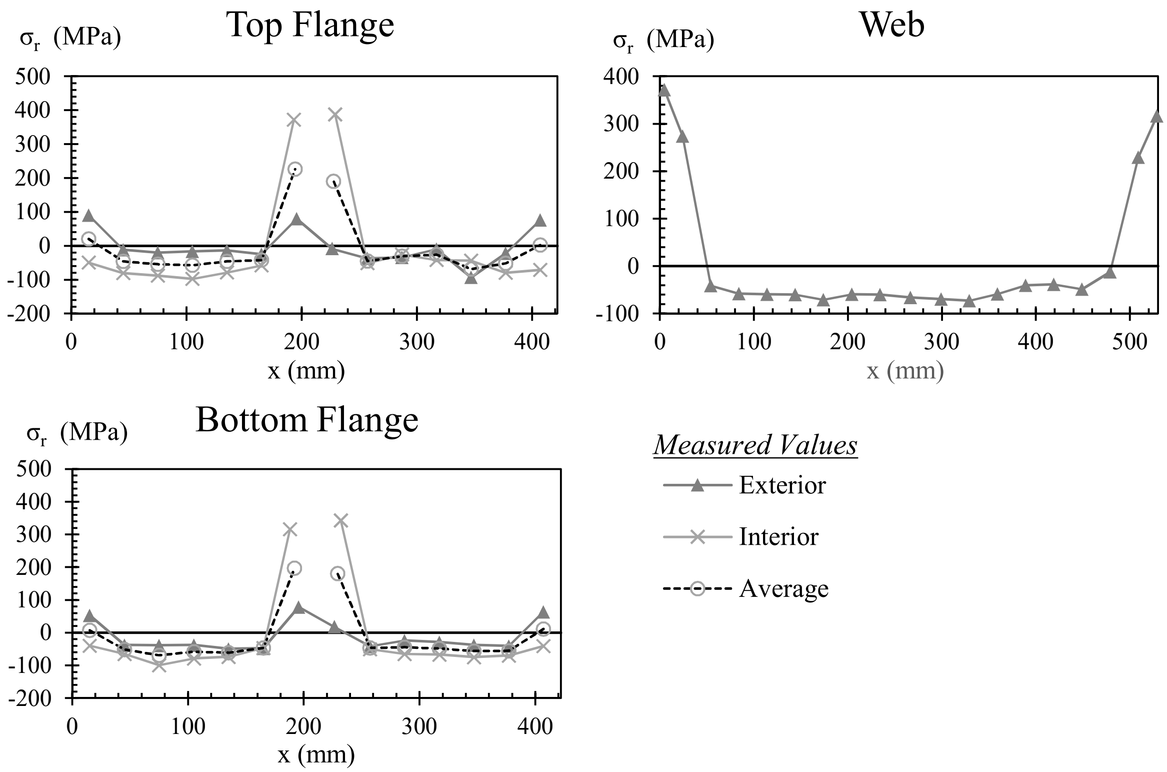

Figure 4: Residual stress distributions from sectioning tests for SP2-2A

4.1.1 Closing Force

In order to confirm the accuracy of results, the total force due to the residual stresses may be summed and the deviation from zero calculated. As residual stresses are internal stresses, in order for equilibrium to be preserved the sum of forces in the longitudinal direction should be equal to zero.

Internal forces are shown in Table 3. Closing error was found to be 1.3% of the magnitude of the total internal force. It is interesting to note that while the top flange is in net tension, the bottom flange is in net compression, owing to the lower peak tensile stress around the weld.

Table 3: Total internal forces for specimen SP2-2A

Plate	*Tensile force (kN)*	*Compressive force (kN)*	*Net internal force (kN)*
Top flange	1291	903	388
Bottom flange	867	993	-126
Web	444	633	-189
Total	2602	2529	73

5 DISCUSSION

5.1 Comparison of results with Cherneko and Kennedy residual stress model

In order to assess the accuracy of the Cherneko and Kennedy (1991) flame-cut (FC) plate residual stress model for modern welded girders, a comparison was done between the measured distribution of SP2-2A and the model (Figure 5). The accuracy of the model in predicting both tensile and compressive stress magnitudes and the width of the high stress gradient area around the weld were examined. Because the model predicts a constant stress through thickness, measured average-through-thickness stresses were used to compare to the model.

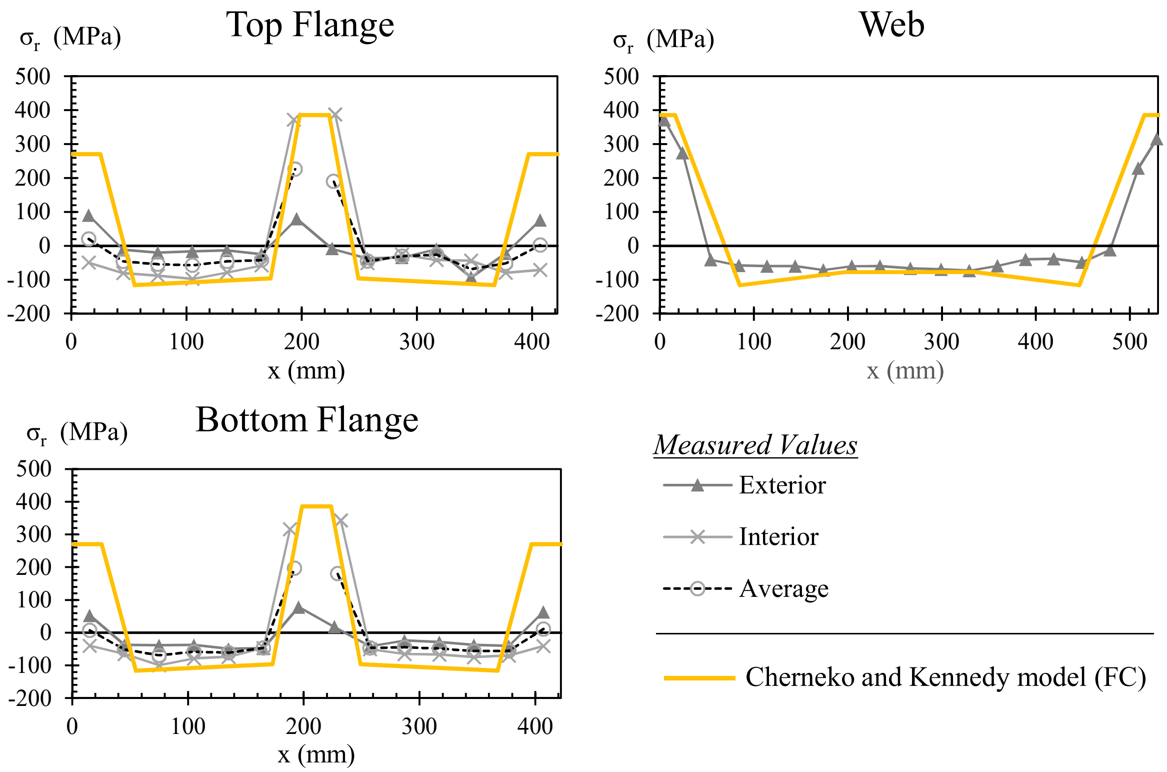

Figure 5: Comparison of Cherneko and Kennedy FC residual stress model with measured values (SP2-2A)

5.1.1 Tensile and compressive stress magnitudes

A significant over-prediction of tensile stress magnitudes in the flanges is observed for specimen SP2-2A (~180-200 MPa). This may be accounted for in part by the difference in yield stress of the base material: the specimens upon which the model is based had a yield stress of 300 MPa whereas the flanges in SP2-2A have a yield stress of 386 MPa. However, even if the yield stress is taken as 300 MPa for the model, the difference will still be substantial (~90-110 MPa). It can be seen from Figure 5, however, that the prediction agrees well with the stress values for the interior face. Because the model applies the same stresses through the entire plate thickness, the prediction may be overly conservative for plates with a significant through-thickness stress gradient (i.e., plates thicker than 1" (Alpsten and Tall 1970)). Compressive stresses in the flanges are also over-predicted by the model, though agreement is closer for the interior face.

Examining the web, it was found that using the flange yield stress for the Cherneko and Kennedy model yields better results than using the web yield stress. Further work will be done to determine the reason for this.

In order to examine the relationship between yield stress and residual stresses, another specimen from the literature of similar flange geometry and fabrication procedure, but with a higher yield stress, was examined (Specimen H1-2018) (Yang et al. 2018). A comparison of material, geometric, and welding information for the two specimens is shown in Table 4. Results are shown in Figure 6.

Table 4: Material, geometric and welding information for specimens SP2-2A and H1-2018 (Yang et al. 2018)

Specimen	σ_{yf} *(MPa)*	σ_{yw} *(MPa)*	b (mm)	t *(mm)*	h *(mm)*	w *(mm)*	*a* *(mm)*	*V* *(V)*	*I* *(A)*	*v* *(mm/s)*
SP2-2A	386	420	422	32	531	13	9	36	500	5.9
H1-2018	481	571	312	25	264	12	10	31-32.5	600-605	4.3

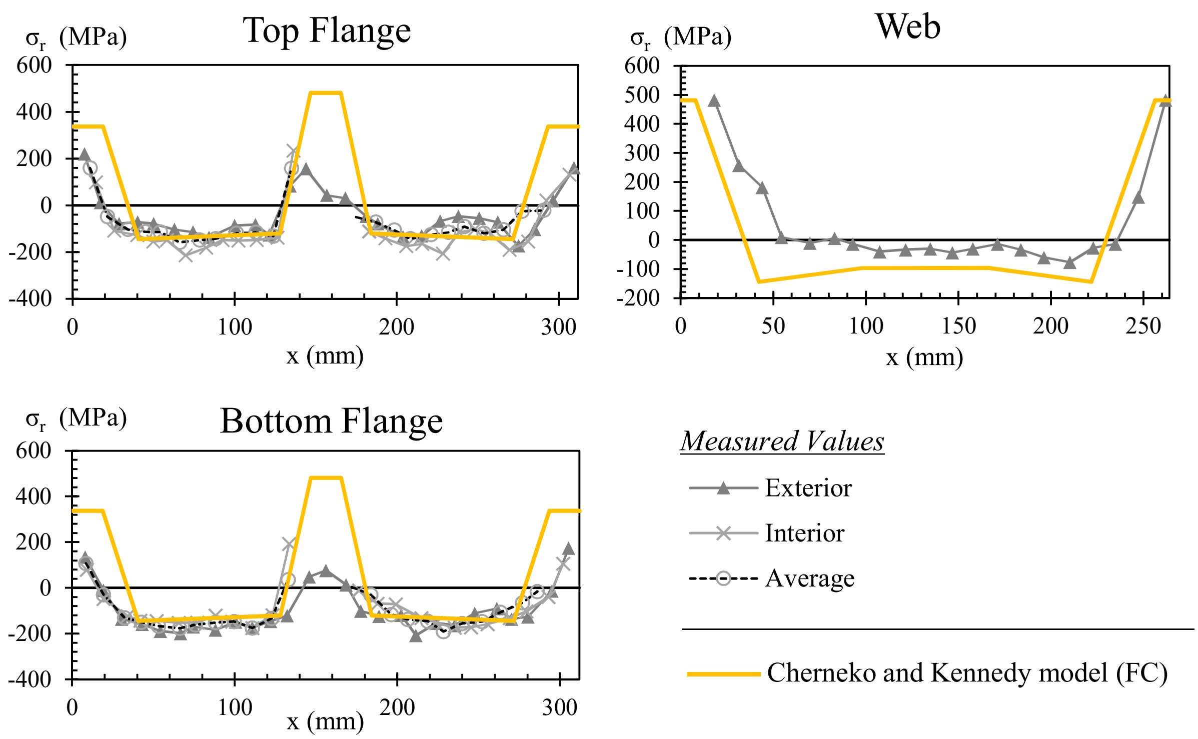

Figure 6: Comparison of Cherneko and Kennedy FC residual stress model with measured values for H1-2018 (Yang et al. 2018)

Peak average tensile stresses in the flanges are lower in specimen H1-2018 than SP2-2A. While it is difficult to draw conclusions from this observation alone (due to the lack of data points around the weld), it does not appear that use of the yield stress as the tensile stress magnitude is accurate for the broader range of specimens: the tensile stress magnitude appears to be influenced by other factors. The same may be said for compressive stress magnitude: excellent agreement is observed for H1-2018, yet a significant over-prediction was found for SP2-2A.

As with SP2-2A, it is observed that use of the flange yield stress gives better results in modelling the web residual stresses. Tensile stress magnitudes were well-predicted, though a greater over-prediction was noted for the compressive stresses when compared to SP2-2A.

5.1.2 High-stress-gradient (tension) zone width

It is not clear if the width of the high-stress-gradient zone around the weld may be considered as a constant fraction of plate width (as the Cherneko and Kennedy model predicts). In order to examine this, a specimen of smaller cross-section (b = 180 mm, t = 10 mm) from a similar study also done by Yang et al. (2016) was examined. A comparison with the Cherneko and Kennedy model is shown in Figure 7.

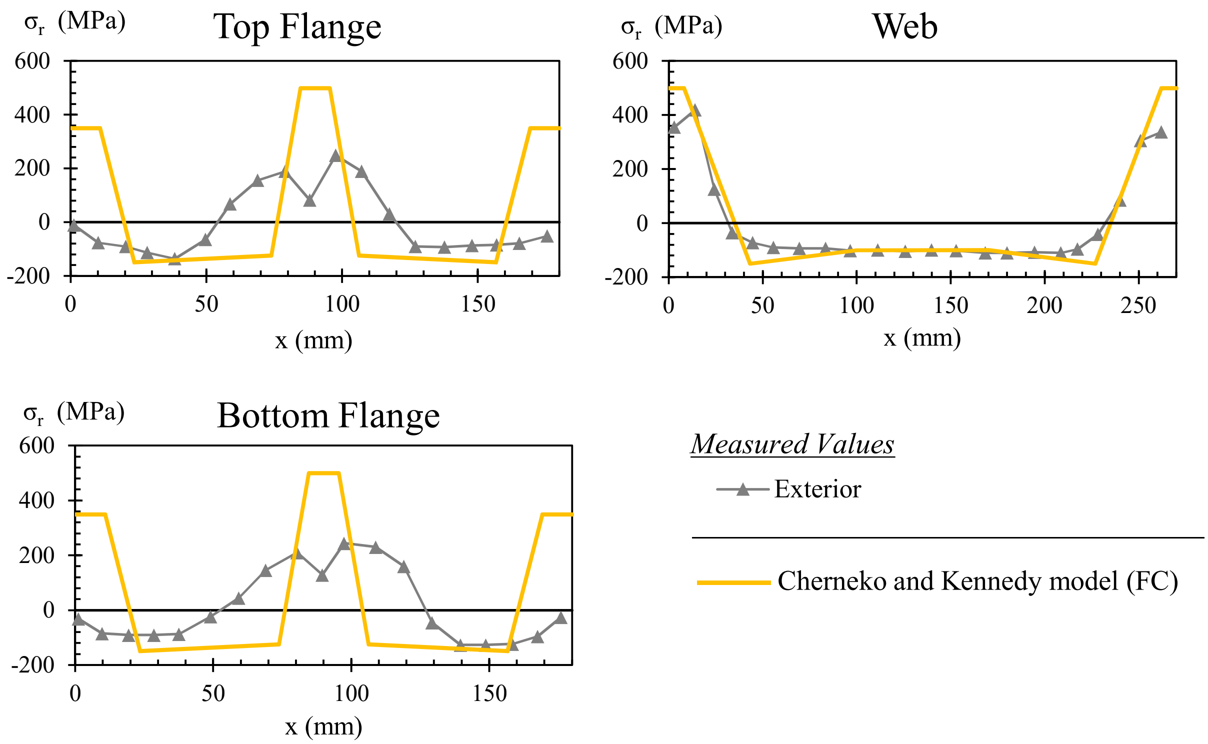

Figure 7: Comparison of Cherneko and Kennedy FC residual stress model measured values for H1 (Yang et al. 2016)

It is seen from Figure 7 that the Cherneko and Kennedy model significantly under-predicts the width of the high-stress-gradient region for specimen H1. This supports the hypothesis that the high-stress-gradient region is not a constant fraction of plate width for welded sections.

It should be noted, however, that agreement between the model and measured distribution is excellent for the web. An examination of several different sections from the literature shows that while the width of the high-stress-gradient region in the flange varies substantially with plate width, that of the web exhibits much less variation and falls relatively close to the value predicted by the Cherneko and Kenndey model, regardless of web height (Figure 8).

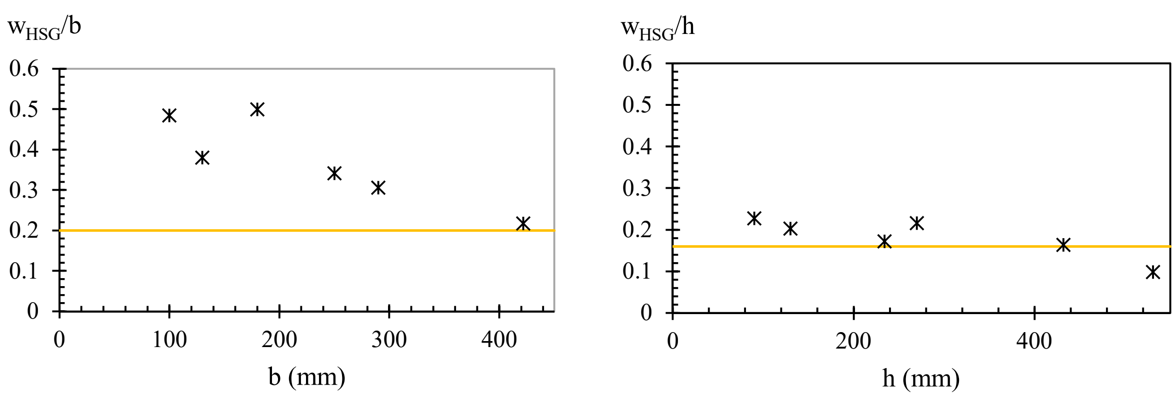

(a) (b)

Figure 8: Normalized weld-induced high-stress-gradient zone width vs. plate width for (a) flanges and (b) webs for a selection of specimens from the literature (see Table 5). Value predicted by Cherneko and Kennedy model in yellow.

Table 5: Selected specimens from the literature

Reference	*ID*	b *(mm)*	t *(mm)*	h *(mm)*	w *(mm)*
Fukumoto and Itoh (1981)	FI-MEAN	100	8	234	6
Ban et al. (2013)	R11-460	130	10	90	10
Ban et al. (2013)	R14-460	290	10	130	10
Yang et al. (2016)	H1	180	10	270	8
Yang et al. (2016)	H8	250	16	432	10

The Fukumoto and Itoh distribution was also used by Kabir and Bhowmick in a finite-element study of LTB for sections with flange widths ranging from 300 – 550 mm. Given the trend of the data in Figure 8a, the Fukumoto and Itoh distribution does not appear to be an accurate representation of such sections.

6 CONCLUSIONS

The sectioning method was used to take residual stress measurements on a welded wide-flange girder fabricated using modern, North-American procedures. Using the sectioning method. Results were then compared to two residual stress distributions from the literature that have seen past use in numerical models. The following conclusions are made:

- While the Cherneko and Kennedy model predicts the tensile stress magnitude for SP2-2A on the interior face of the flange with reasonable accuracy, measured stresses are substantially lower on the exterior face. Because the model applies the same stresses through the entire plate thickness, the model over-estimates tensile stress magnitudes significantly.
- Compressive stresses in the flanges are over-predicted by the Cherneko and Kennedy model for SP2-2A.
- Peak tensile stress magnitude in the web is closer to the flange yield stress than the web yield stress.
- The width of the high-stress-gradient zone induced by welding is not a constant fraction of plate width in the flanges. The Cherneko and Kennedy model is derived from sections with 300 – 400 mm wide flanges and will not yield accurate distributions for sections with narrower flanges. The width of this zone in webs exhibits much less variation with plate width and can be reasonably approximated by the Cherneko and Kennedy model.
- The distribution measured by Fukumoto and Itoh is not accurate for larger sections as the high-stress-gradient region is not a constant fraction of flange width.

ACKNOWLEDGEMENTS

This research is funded by the Natural Sciences and Engineering Research Council of Canada and the CISC Centre for Steel Structures Education and Research at the University of Alberta. The authors would like to acknowledge SSAB for donation of the steel for this project and Supreme Steel LP for specimen fabrication and design assistance.

REFERENCES

Alpsten, G.A., and Tall, L. 1970. Residual Stresses in Heavy Welded Shapes. *Welding Research Supplement*, **49**(3): 93–105.

Chernenko, D.E., and Kennedy, D.J.L. 1991. An Analysis of the Performance of Welded Wide Flange Columns. *Canadian Journal of Civil Engineering*, **18**(4): 537–55. https://doi.org/10.1139/l91-067.

Canadian Standards Association (CSA). 2014a. Canadian Highway Bridge Design Code. CAN/CSA-S6-14.

Canadian Standards Association (CSA). 2014b. Limit States Design of Steel Structures. CAN/CSA-S16-14.

Fukumoto, Y., and Itoh, Y. 1981. Statistical Study of Experiments on Welded Beams. *Journal of the Structural Division, ASCE*, **107**(ST1): 89–103.

Fukumoto, Y., Yoshito, I., and Kubo, M. 1980. Strength Variation of Laterally Unsupported Beams. *Journal of the Structural Division, ASCE*, **109**(ST1): 541–62.

Kabir, I., and Bhowmick, A.K. 2018. Lateral Torsional Buckling of Welded Wide Flange Beams. *Canadian Journal of Civil Engineering*, **45**(9): 766–79.

Kalakoutsky, N. 1888. The Study of Internal Stresses in Cast Iron and Steel. *London*,.

MacPhedran, I., and Grondin, G.Y. 2011. A Simple Steel Beam Design Curve. *Canadian Journal of Civil Engineering*, **38**: 141–53. https://doi.org/10.1139/L10-114.

Pekoz, T., Bjorhovde, R., Errera, S.J., Johnston, B.G., Sherman, D.R., and Tall, L. 1981. Determination of Residual Stresses in Structural Shapes. *Experimental Techniques*, **5**(3): 4–7.

Tebedge, N., Alpsten, G., and Tall, L. 1973. Residual-Stress Measurement by the Sectioning Method. *Experimental Mechanics*, **13**(2): 88–96. https://doi.org/10.1007/BF02322389.

Yang, B., Nie, S., Xiong, G., Hu, Y., Bai, J., Zhang, W., and Dai, G. 2016. Residual Stresses in Welded I-Shaped Sections Fabricated from Q460GJ Structural Steel Plates. *Journal of Constructional Steel Research*, **122**: 261–73. https://doi.org/10.1016/j.jcsr.2016.03.029.

Yang, B., Xiong, G., Nie, S., Elchalakani, M., and Zhu, Q. 2018. Experimental and Model Investigation on Residual Stresses in Q460GJ Thick-Walled I-Shaped Sections. *Journal of Constructional Steel Research*, **145**: 489–503. https://doi.org/10.1016/j.jcsr.2018.03.008.